

Novel vibrational resonance in multistable systems

S. Rajasekar,^{1,a)} K. Abirami,¹ and M. A. F. Sanjuan^{2,b)}

¹*School of Physics, Bharathidasan University, Tiruchirappalli, Tamilnadu 620 024, India*

²*Departamento de Física, Universidad Rey Juan Carlos, Tulipán s/n, 28933 Móstoles, Madrid, Spain*

(Received 11 May 2011; accepted 22 June 2011; published online 29 July 2011)

We investigate the role of multistable states on the occurrence of vibrational resonance in a periodic potential system driven by both a low-frequency and a high-frequency periodic force in both underdamped and overdamped limits. In both cases, when the amplitude of the high-frequency force is varied, the response amplitude at the low-frequency exhibits a series of resonance peaks and approaches a limiting value. Using a theoretical approach, we analyse the mechanism of multiresonance in terms of the resonant frequency and the stability of the equilibrium points of the equation of motion of the slow variable. In the overdamped system, the response amplitude is always higher than in the absence of the high-frequency force. However, in the underdamped system, this happens only if the low-frequency is less than 1. In the underdamped system, the response amplitude is maximum when the equilibrium point around which slow oscillations take place is maximally stable and minimum at the transcritical bifurcation. And in the overdamped system, it is maximum at the transcritical bifurcation and minimum when the associated equilibrium point is maximally stable. When the periodicity of the potential is truncated, the system displays only a few resonance peaks.

© 2011 American Institute of Physics. [doi:10.1063/1.3610213]

The analysis of the effects of two-frequency signals is of great importance in physics, engineering, and biology. Landa and McClintock¹ have shown that the response of a nonlinear system to the low-frequency periodic signal passes through a maximum depending on the amplitude of an additional high-frequency signal. The point is that frequencies far from them can cause a resonance phenomenon which is termed as vibrational resonance (VR). The phenomenon of VR has been studied in single-, double-, and triple-well and also in excitable systems. As a consequence of this analysis, it becomes very important to study the different kinds of nonlinear systems from either the understanding of the very nature of VR or its possible applications. The objective of the present work is precisely to explore what kind of features presents the phenomenon of VR in periodic potential systems and, in particular, in the pendulum system in both the underdamped and the overdamped cases. The equation of motion of the pendulum system constitutes a paradigmatic model in the explorations of bifurcations, chaos, and diffusion phenomena of many nonlinear dynamical systems. Here, we perform our investigation of the VR for the pendulum from a theoretical point of view and verify the theoretical predictions by numerical simulations.

phenomenon was first reported by Landa and McClintock.¹ Its subsequent analysis has received much attention in the past few years because of its importance in a wide variety of contexts in physics, engineering, and biology.^{2–7} Theoretical approaches have been developed to study VR.^{6,8,9} The occurrence of VR has been studied in a monostable,¹⁰ bistable,^{1,8,9,11,12} and three well¹³ systems. Moreover, it has been also analyzed in excitable systems,¹⁴ vertical cavity surface emitting laser,^{15,16} coupled oscillators,^{4,17,18} and time-delay systems.^{19–22} Very recently, VR is found to induce undamped low-frequency signal propagation in one-way coupled¹⁷ and globally coupled²³ bistable systems. Vibrational ratchet motion is studied in certain systems with spatially periodic potentials driven by a biharmonic force and a Gaussian white noise.²⁴ In the pendulum system driven by a high-frequency periodic force and noise, employing vibrational mechanics scheme, it has been shown that mobility and diffusion coefficient are extremely sensitive to mass even for large damping.²⁵

It is appropriate to note here that when the second high-frequency periodic force in a typical bistable system is replaced by a noise term, the resultant resonance is the well-known stochastic resonance (SR).²⁶ There are similarities and differences between SR and VR. Both SR and VR were often studied in systems with nonperiodic potentials. However, very little work has been done on SR in periodic potentials.^{27–29} In the pendulum system, it is shown²⁷ that the exhibited resonant behaviour is not the SR associated with the hopping between the wells, but it is a noise enhanced resonance due to the intra-well motion. Furthermore, and due to the diffusion dynamics, there is no synchronization of the dynamical variable and the periodic driving force. Very recently, SR has been analysed²⁸ in a potential with an arbitrary number of maxima and minima. By applying a linear

I. INTRODUCTION

The phenomenon of vibrational resonance (VR) is a dynamical resonance induced by a high-frequency periodic force at the low-frequency ω of the input periodic signal. This

^{a)}Electronic mail: rajasekar@cndd.bdu.ac.in.

^{b)}Electronic mail: miguel.sanjuan@urjc.es.

response theory, it is obtained an optimal number of maxima and minima for which the response is maximized. Now, a natural question arises: Can a biharmonic signal give rise to VR in periodic potential systems? The main goal of the present work is precisely to investigate, through a theoretical approach and numerical simulation, the occurrence and the features of VR in the pendulum system for both underdamped and overdamped cases driven by the biharmonic force $f \cos \omega t + g \cos \Omega t$.

The equations of motion of the underdamped and overdamped pendulum systems are

$$\ddot{\theta} + d\dot{\theta} + \sin \theta = f \cos \omega t + g \cos \Omega t \quad (1)$$

and

$$\dot{\theta} + \sin \theta = f \cos \omega t + g \cos \Omega t, \quad (2)$$

respectively. The equation of motion of the pendulum system also describes the dynamics of several physical systems including rf-driven Josephson junctions and phase-locked voltage-controlled oscillators. In Eqs. (1) and (2), we assume that $\Omega \gg \omega, f, g > 0$, and $f \ll 1$. The amplitudes f and g can differ in orders of magnitude. Such mixed signals have been used in different fields of science and engineering. Examples include a two-frequency laser signal showing high stability and high efficiency,² an acoustic field consisting of a high-frequency imaging wave and a low-frequency audio pumping wave⁴ found to be useful for measuring changes in the fluid pressure³⁰ and distinguish size distributions of gas filled micro-pores,³¹ and an injection current used in a vertical cavity surface emitting laser for experimental demonstration of VR,¹⁵ telecommunication signals where information carriers are usually high-frequency waves modulated by a low-frequency signal³² and ultrasonic two-frequency waves used to enhance cavitation yield.³³

In the absence of periodic forcing and damping, the potential of the pendulum system is $V(\theta) = -\cos \theta$. This potential has minima at $\theta_{\min}^* = \pm 2n\pi$, $n = 0, 1, 2, \dots$ and maxima at $\theta_{\max}^* = \pm(2n+1)\pi$, $n = 0, 1, 2, \dots$. Furthermore, θ_{\min}^* and θ_{\max}^* are the stable and unstable equilibrium points, respectively, of the system. For $\Omega \gg \omega$, it is reasonable to assume that the solution of the system consists of both a slow variable X and a fast variable ψ . Substituting $\theta = X + \psi$ in Eq. (1), we obtain coupled equations for the variables X and ψ . Because ψ is a rapidly changing, we approximate its equation of motion as a damped and periodically driven (by the high-frequency force) free particle whose solution in the long time limit is a periodic function of fast time $\tau = \Omega t$. On averaging out $\psi(\tau)$ over the period of the fast time, we obtain the nonlinear equation of motion for the slow variable X . For $f \ll 1$, we assume that the amplitude of the slow oscillation is small and consider linearized equation of motion of X . This leads to, in the linear approximation, an analytical expression for the amplitude (denoted as A_L) of slow motion. In a similar manner, we find an expression for A_L of slow motion for the system (2). The ratio of A_L and f is termed as response amplitude Q . Using the theoretical expression of Q , we analyze the occurrence of VR in both underdamped and overdamped systems.

The organization of the paper is as follows. In Sec. II, we obtain the equation of motion of the slow variable X and an approximate theoretical expression for the response amplitude Q for the underdamped system (Eq. (1)). We show the occurrence of multiple VR and bring out the differences between the VR in the pendulum system and other systems with nonperiodic potentials. We analyse the resonance dynamics in terms of the resonant frequency ω_r and the stability of equilibrium points around which slow oscillations take place. We consider the overdamped system (Eq. (2)) in Sec. III. In Sec. IV, we study the effect of the truncation of the periodicity of the potential. Finally, the conclusions are described in Sec. V.

II. UNDERDAMPED PENDULUM SYSTEM

The first objective is to find a solution of Eq. (1) for $\Omega \gg \omega$ by the method of separation where the solution is written as a sum of slow variable $X(t)$ and fast variable $\psi(t, \Omega t)$: $\theta(t) = X(t) + \psi(t, \Omega t)$. We assume that X is periodic with period $2\pi/\omega$ and ψ is periodic in the fast time $\tau = \Omega t$ with period 2π . Substituting $\theta = X + \psi$ into Eq. (1), we obtain

$$\ddot{X} + \ddot{\psi} + d(\dot{X} + \dot{\psi}) + \cos \psi \sin X + \sin \psi \cos X = f \cos \omega t + g \cos \Omega t. \quad (3)$$

Due to the presence of the mixed terms $\cos \psi \sin X$ and $\sin \psi \cos X$, we add and subtract the terms $\langle \cos \psi \rangle \sin X$ and $\langle \sin \psi \rangle \cos X$, where

$$\langle \cos \psi \rangle = \frac{1}{2\pi} \int_0^{2\pi} \cos \psi(\tau) d\tau, \quad \langle \sin \psi \rangle = \frac{1}{2\pi} \int_0^{2\pi} \sin \psi(\tau) d\tau \quad (4)$$

with $\langle F(t) \rangle$ representing the average value of $F(t)$ over $\tau = 0$ to 2π in Eq. (3) and obtain the following equations for X and ψ :

$$\ddot{X} + d\dot{X} + \langle \cos \psi \rangle \sin X + \langle \sin \psi \rangle \cos X = f \cos \omega t, \quad (5)$$

$$\ddot{\psi} + d\dot{\psi} + [\cos \psi - \langle \cos \psi \rangle] \sin X + [\sin \psi - \langle \sin \psi \rangle] \cos X = g \cos \Omega t. \quad (6)$$

Essentially, because ψ is assumed to be rapidly oscillating periodic function of fast time, the terms containing ψ in the evolution equation of X are averaged out over its period and, moreover, Eq. (6) can be approximated as^{24,25}

$$\ddot{\psi} + d\dot{\psi} = g \cos \Omega t. \quad (7)$$

A. Approximate theoretical expression for the response amplitude Q

The solution of Eq. (7) in the long time limit is²⁵ $\psi = \mu \cos(\Omega t + \phi)$ where $\mu = g/(\Omega \sqrt{\Omega^2 + d^2})$ and $\phi = \tan^{-1}(d/\Omega)$. Then, we find $\langle \cos \psi \rangle = J_0(\mu)$ and $\langle \sin \psi \rangle = 0$ where $J_0(\mu)$ is the zeroth-order Bessel function. Throughout our analysis on underdamped system, we choose $\Omega \gg d$. In this case, we can neglect d^2 in the argument of $J_0(\mu)$ and approximate it as $J_0(g/\Omega^2)$. Now, Eq. (5) becomes

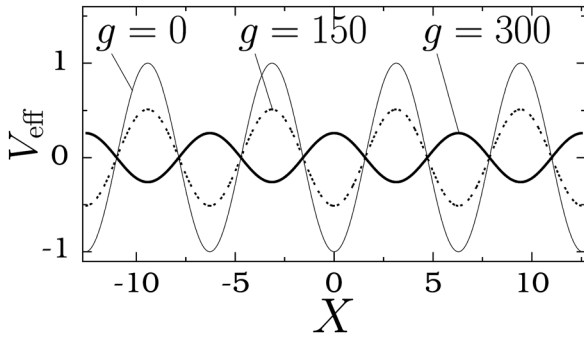


FIG. 1. Plot of the effective potential V_{eff} given by Eq. (9) for three values of g with $\Omega = 10$. Notice that for $g = 0$ and $g = 150$, the shapes of the potential remain the same while the depth of the wells is reduced, showing the effect of the value of g .

$$\ddot{X} + d\dot{X} + J_0(g/\Omega^2) \sin X = f \cos \omega t. \quad (8)$$

If $\Omega \gg d$ is not the case, then $J_0(g/\Omega^2)$ in the above equation must be replaced by $J_0(\mu)$. Equation (8) can be treated as a forced motion of a particle in the effective potential,

$$V_{\text{eff}}(X) = -J_0(g/\Omega^2) \cos X. \quad (9)$$

In Fig. 1, we plotted the effective potential $V_{\text{eff}}(X)$ for a few values of g with $\Omega = 10$. We can clearly notice the effect of g . For $g = 0$ and 150, the shapes of the potential remain the same while the depth of the wells is reduced. The maxima and minima of V_{eff} are altered by the parameter g . The maxima and the minima of V_{eff} for $g = 0$ and 150 become the minima and maxima for $g = 300$. Figure 2 shows $J_0(g/\Omega^2)$ versus g for $\Omega = 10$. Here, we can see that J_0 oscillates around the value 0 with decreasing amplitude and $J_0 \rightarrow 0$ as $g \rightarrow \infty$. Whenever $J_0 > 0$, the minima of V_{eff} are $X_{\text{min}}^* = \pm 2n\pi$, $n = 0, 1, 2, \dots$ and the maxima are $X_{\text{max}}^* = \pm (2n + 1)\pi$, $n = 0, 1, 2, \dots$. The locations of the minima and the maxima of V_{eff} are interchanged when $J_0 < 0$. A consequence of this is that for the values of g for which $J_0 > 0$ slow oscillations occur around the equilibrium points $(X^*, \dot{X}^*) = (X_{\text{min}}^*, 0)$, while for other values they take place around $(X^*, \dot{X}^*) = (X_{\text{max}}^*, 0)$.

The equation of motion for the deviation variable $Y = X - X^*$ is given by

$$\ddot{Y} + d\dot{Y} + (J_0 \cos X^*) \sin Y = f \cos \omega t. \quad (10)$$

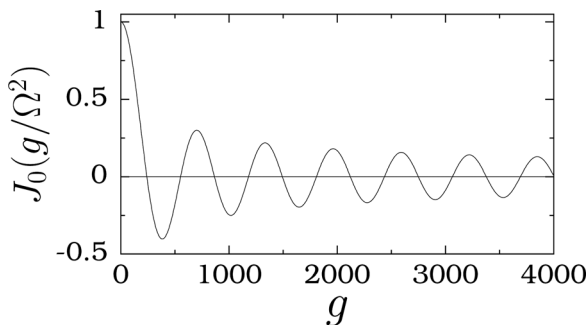


FIG. 2. Variation of the zeroth-order Bessel function with the control parameter g for $\Omega = 10$. Note that J_0 exhibits a damped oscillation. Moreover, the values of g at which $J_0 = 0$ are not equally spaced.

If $J_0 > 0$ (< 0), then $X^* = X_{\text{min}}^*$ (X_{max}^*). Therefore, $J_0 \cos X^* = |J_0|$. For $f \ll 1$, we assume that $|Y| \ll 1$ and approximate $\sin Y$ as Y . Then Eq. (10) becomes

$$\ddot{Y} + d\dot{Y} + \omega_r^2 Y = f \cos \omega t, \quad \omega_r^2 = |J_0|, \quad (11)$$

which is a damped and periodically driven linear equation. We note that ω_r is the natural frequency of the linear version of the equation of motion of the slow variable X in the absence of the external force $f \cos \omega t$. It is called resonant frequency of the low-frequency oscillation in the presence of $f \cos \omega t$. ω_r is independent of f , ω , and d and depends on the parameters g and Ω . Below we show that resonance occurs when the resonant frequency matches with the angular frequency ω or it becomes locally maximum. The general solution of Eq. (11) is

$$Y(t) = C_1 e^{m_+ t} + C_2 e^{m_- t} + A_L \cos(\omega t + \Phi), \quad (12)$$

where C_1 and C_2 are integration constants, m_{\pm} are the roots of the equation $m^2 + dm + \omega_r^2 = 0$, and

$$A_L = \frac{f}{\sqrt{S}}, \quad S = (\omega_r^2 - \omega^2)^2 + d^2 \omega^2, \quad (13a)$$

$$\Phi = \tan^{-1}[-d\omega/(\omega_r^2 - \omega^2)]. \quad (13b)$$

The roots m_{\pm} are < 0 for $d^2 > 4\omega_r^2$ and become complex conjugate with negative real part for $d^2 < 4\omega_r^2$. Consequently, in the limit $t \rightarrow \infty$, the first two terms in the solution (12) falls-off exponentially fast to zero and are termed as transient. The last term in Eq. (12) is the dominant component of the solution. Therefore, for large t , we write the solution as $Y(t) = A_L \cos(\omega t + \Phi)$. Finally, the response amplitude is given by $Q = A_L/f = 1/\sqrt{S}$.

B. Analysis of VR: Connection between resonance and ω_r

In order to verify theoretical results, we numerically integrate Eq. (1) using the fourth-order Runge-Kutta method with step size $(2\pi/\omega)/1000$ and leave the solution corresponding to first 1000 drive cycles of low-frequency force as a transient. Then, we compute numerically the sine and cosine components Q_S and Q_C , respectively from the equations

$$Q_S = \frac{2}{kT} \int_0^{kT} \theta(t) \sin \omega t dt, \quad (14a)$$

$$Q_C = \frac{2}{kT} \int_0^{kT} \theta(t) \cos \omega t dt, \quad (14b)$$

where $T = 2\pi/\omega$ and $k = 500$. Then $Q = \sqrt{Q_S^2 + Q_C^2}/f$. For the purposes of our analysis, we treat g as the control parameter. Figure 3 shows both theoretical and numerical values of Q versus g for four set of values of ω and Ω with $f = 0.1$ and $d = 1$. The theoretical prediction is in a very close agreement with the numerical simulation. There are several interesting results on the pendulum system compared to the VR reported on the other systems with nonperiodic potentials.

First, we note that the values of g , g_{VR} , at which Q becomes maximum (i.e., S becomes minimum), are the roots

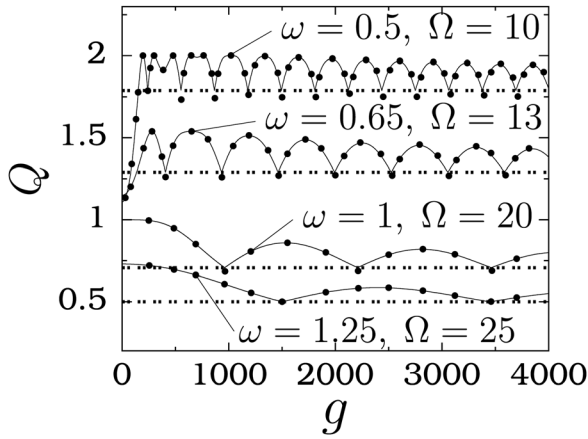


FIG. 3. Response amplitude Q versus the control parameter g for the underdamped pendulum system for a few set of values of ω and Ω . The values of d and f are 1 and 0.1, respectively. The continuous curve and the solid circles represent the theoretical Q and the numerically computed Q , respectively. The dashed horizontal lines indicate the limiting values of Q .

of the equation $S_g = dS/dg = J_{0g}(|J_0| - \omega^2) = 0$ with $J_{0g} = dJ_0/dg$ where we have used $\omega_r^2 = |J_0|$. Therefore, resonance occurs if $|J_0| = \omega^2$ or $J_{0g} = 0$. We note that $J_0(0) = 1$, $|J_0(g/\Omega^2)| < 1$ and it oscillates around the value 0 with a decreasing amplitude. Suppose g_c is the value of g above which $|J_0|$ is always $< \omega^2$. Then for $g < g_c$, the values of g at which resonance occurs are the roots of $|J_0| - \omega^2 = 0$. For $g > g_c$, the resonance values of g are the roots of the equation $J_{0g} = 0$. These are clearly seen in Fig. 4 which shows the connection between the resonances and ω_r^2 for $\omega = 0.5$ and $\Omega = 10$. The value of g_c is 761, however, the values of g_{VR} are not equally spaced.

Since $|J_0| < 1$, we find from $Q = 1/\sqrt{S}$ that for $\omega \geq 1$ $Q(g) < Q(g=0)$. That is, there is no gain in the response am-

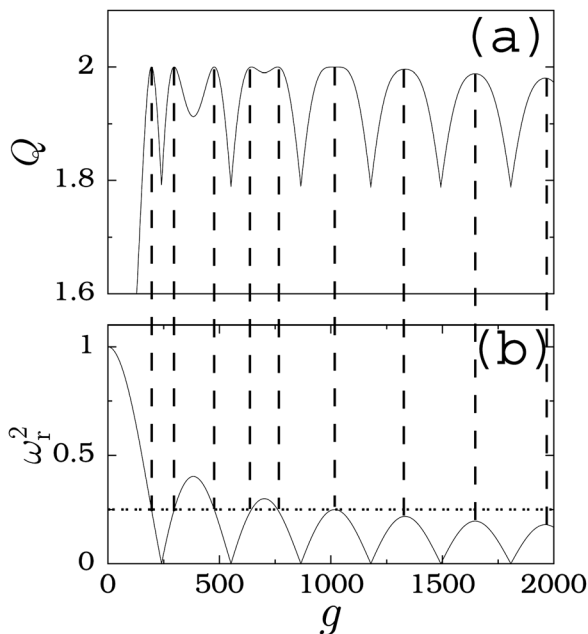


FIG. 4. Plots of (a) Q versus g and (b) $\omega_r^2 (= |J_0(g/\Omega^2)|)$ versus g for the underdamped pendulum system with $\omega = 0.5$, $\Omega = 10$, $f = 0.1$, and $d = 1$. In (b), the horizontal dashed line denotes $\omega_r^2 = \omega^2 = 0.25$. The vertical dashed lines indicate the values of ω_r^2 and g at which Q becomes maximum.

plitude at the frequency $\omega \geq 1$ due to the addition of a high-frequency force. However, due to the damped oscillatory variation of J_0 , the response amplitude Q will show an oscillatory variation and it becomes maximum whenever $|J_0|$ is maximum (i.e., $J_{0g} = 0$). The above results are clearly evident in Fig. 3 for $\omega = 1$ and 1.25.

For $\omega < 1$, a key result is $Q(g) > Q(g=0)$. At the resonances occurring for $g < g_c$, $Q_{max} = 1/(d\omega)$. At other resonances ($g_{VR} > g_c$), which are due to the local maxima of ω_r^2 (see Figs. 3 and 4), the value of Q_{max} slowly decreases from the value $1/(d\omega)$ and approaches the limiting value Q_L (indicated by dashed lines in Fig. 3) in the limit of $g \rightarrow \infty$. These results are clearly seen in Figs. 3 and 4.

An interesting result, for both $\omega > 1$ and $\omega < 1$, is that Q does not decay to 0, whereas in the systems with a finite number of potential wells $Q \rightarrow 0$ for sufficiently large values of g because of the monotonic increase of the resonant frequency for large values of g .^{1,8,10,12,13} In the pendulum system, since $\omega_r^2 = |J_0| \rightarrow 0$ as $g \rightarrow \infty$, the limiting value of Q for large values of g is $Q_L = 1/(\omega\sqrt{\omega^2 + d^2})$. As g increases, the strength of the effective potential seen by the slow variable decreases (see Fig. 1), and for sufficiently large values of g , the equation of motion of a periodically driven damped free particle (Eq. (8) with $J_0 = 0$), and in this case, the response amplitude is Q_L .

Next, we present the effect of the angular frequency Ω on VR. Figure 5 shows the variation of Q as a function of Ω for $g = 100$. Multiresonance occurs when Ω is varied. The differences between the effects of Ω and g on VR can be easily noticed by comparing the Figs. 3 and 5. For large values of Ω , $g/\Omega^2 \approx 0$, $J_0(g/\Omega^2) \approx 1$, and Q approaches the limiting value $1/\sqrt{(1 - \omega^2)^2 + d^2\omega^2}$ which is $Q(g=0)$, whereas for large values of g , $Q \approx Q_L = 1/(\omega\sqrt{\omega^2 + d^2})$. On the other

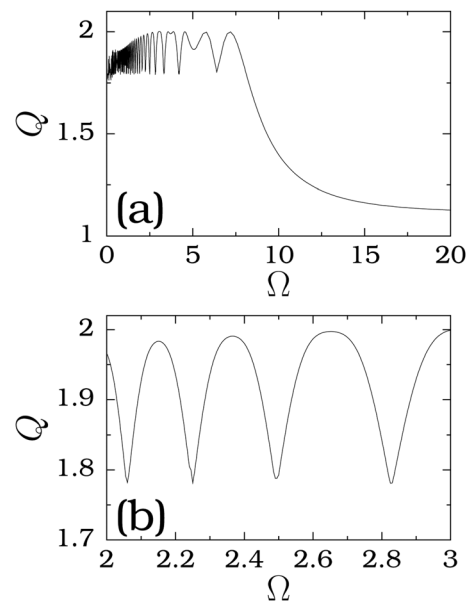


FIG. 5. Numerically computed Q versus Ω for the underdamped system with $f = 0.1$, $d = 1$, $\omega = 0.5$, and $g = 100$. The subplot (b) is a magnification of a part of Q in (a).

hand, for small values of Ω , $\omega_r^2 = J_0(g/\Omega^2)$ oscillates very fast (because $1/\Omega^2$ varies rapidly) and hence, Q also oscillates fast and is clearly seen in Figs. 5(a) and 5(b). The spacing between successive resonances decreases rapidly when Ω is decreased from a higher value.

In our study, we treated $f \ll 1$. In Fig. 3, for $\omega = 0.5$ and $\Omega = 10$, the first resonance occurs at a large value of g . Resonance can be observed for lower values of g also by choosing smaller values for ω and Ω . For example, for $\Omega = 10$ and 5, the first resonance occurs at $g = 195.5$ and 48.87, respectively. Further, resonance with considerable enhancement of response amplitude of the output signal of the system at the low frequency ω occurs only for small values of f . For several fixed values of $f (< 100)$, we calculated Q for a range of values of g of same order of magnitude of f . In all the cases, the variation of Q with g is found to be negligibly small. When $f = 0$, the system (1) is now driven by only one periodic force with angular frequency Ω and amplitude g . In this case, the system can exhibit different routes to chaos and chaotic diffusion when g or Ω is varied. We obtained a theoretical frequency-response amplitude equation for $0 < g \ll 1$ by assuming the solution of the form $A \cos(\Omega t + \phi)$. For a certain range of fixed values of the damping parameter, the response amplitude follows different paths (hysteresis) when Ω is increased from a small value to a large value and decreased from a large value to a small value and single resonance occurs. Multiresonance phenomenon is not observed.

In the VR analysis, we assume that there is a periodic signal with frequency ω and very low amplitude $f \ll 1$. Interestingly, VR analysis indicates that when this low amplitude signal is fed to a nonlinear system driven by a second periodic force of frequency Ω far from ω , $\Omega \gg \omega$, then the amplitude of the output signal at the frequency ω can be maximized by an appropriate amplitude g of the high-frequency force. This high-frequency force induced VR is of great interest for the detection of low level signal.

C. Analysis of VR: Connection between resonance and stability of the equilibrium points

Now, we bring out the connection between the VR and the stability of the equilibrium points around which slow oscillations take place. The equilibrium points of the system (Eq. (8)) for $f = 0$ are $(X_{min}^*, \dot{X}^*) = (\pm 2n\pi, 0)$, $n = 0, 1, 2, \dots$ and $(X_{max}^*, \dot{X}^*) = (\pm (2n + 1)\pi, 0)$, $n = 0, 1, 2, \dots$. The stability determining eigenvalues are

$$\lambda_{\pm} = \frac{1}{2} \left[-d \pm \sqrt{d^2 - 4J_0 \cos X^*} \right]. \tag{15}$$

If $J_0 > 0$, then for $(X_{min}^*, 0)$, $\text{Re}\lambda_{\pm} < 0$ and are stable, while for $(X_{max}^*, 0)$, λ_{\pm} are real with $\lambda_+ > 0$ while $\lambda_- < 0$ and are unstable (saddles). The stability is exchanged for $J_0 < 0$. That is, the stability of the equilibrium points is changed when g is varied and the associated bifurcation is the transcritical bifurcation. A consequence of this is that for the values of g for which $J_0 > 0$ slow oscillations occur around the equilibrium points $(X_{min}^*, 0)$, while for other values, they

take place around $(X_{max}^*, 0)$. Around each of the stable equilibrium points, there exists a slow orbit. The coexisting slow orbits and the coexisting actual orbits can be obtained by choosing different initial conditions in the numerical simulation.

Figures 6(a) and 6(c) show the variation of $\text{Re}\lambda_{\pm}$ of $(X_{min}^*, 0)$ and $(X_{max}^*, 0)$, respectively. As g increases from zero, the eigenvalues of $(X_{min}^*, 0)$ are complex conjugate with a negative real part, while for $(X_{max}^*, 0)$, we find $\lambda_- < 0 < \lambda_+$. The imaginary part of λ_{\pm} of $(X_{min}^*, 0)$ decreases in magnitude and at a value of g , they are pure real negative. Then at another value of g , one of the eigenvalues of $(X_{min}^*, 0)$ becomes positive (while those of $(X_{max}^*, 0)$ become complex conjugate with negative real part). At this value of g , the stability of $(X_{min}^*, 0)$ and $(X_{max}^*, 0)$ are exchanged and the associated bifurcation is transcritical. The transcritical bifurcation repeats as g increases. Q attains the limiting value Q_L at the transcritical bifurcation points. Resonances occur when $(X_{min}^*, 0)$ or $(X_{max}^*, 0)$ are maximally stable, i.e., the real part of the largest eigenvalue is minimum. These can be clearly seen in Fig. 6.

In Fig. 7, we plotted θ^* (the θ -component of the equilibrium point about which both slow as well as the actual oscillations occur) versus g along with the response amplitude Q . Comparing Figs. 2 and 7, we find that the center of

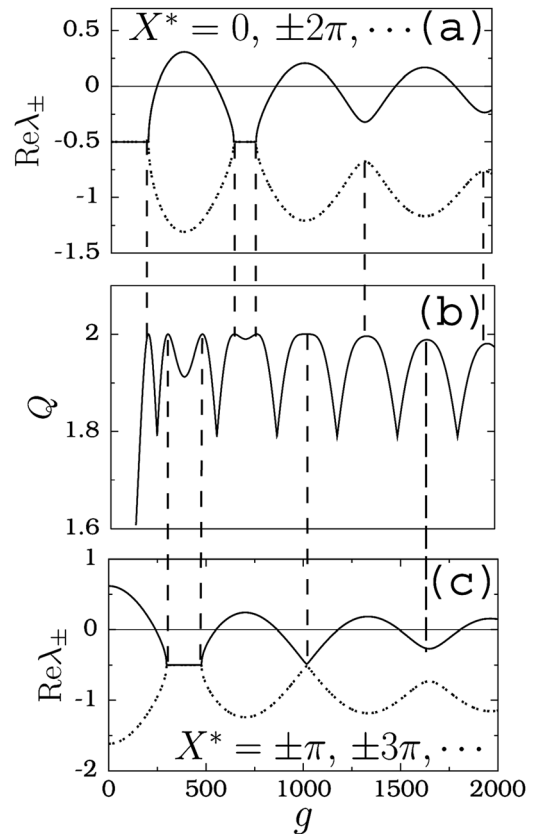


FIG. 6. $\text{Re}\lambda_{\pm}$ versus the control parameter g of (a) the equilibrium points $(X_{min}^*, 0)$ and (c) the equilibrium points $(X_{max}^*, 0)$. Continuous and dashed curves represent $\text{Re}\lambda_+$ and $\text{Re}\lambda_-$, respectively. (b) Q versus g of the underdamped pendulum system for $d = 1, f = 0.1, \omega = 0.5$, and $\Omega = 10$. The vertical dashed lines indicate the connection between the resonance and the nature of the eigenvalues of the stable equilibrium points.

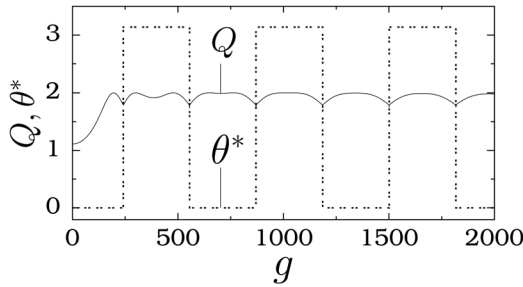


FIG. 7. Response amplitude Q and θ^* (the θ -component of the equilibrium point around which both slow as well as the actual oscillations occur) versus the parameter g for $d=1, f=0.1, \omega=0.5$, and $\Omega=10$.

oscillation switches from $\theta^*=0$ to π and π to 0 when J_0 changes its sign from positive to negative and negative to positive, respectively. The switching takes place not at the resonance but at the transcritical bifurcation point.

III. OVERDAMPED PENDULUM SYSTEM

In this section, we consider the overdamped pendulum system (Eq. (2)). Multiresonance is also realized in the overdamped pendulum system, however, there are some differences in the mechanism of VR.

For the system (Eq. (2)), we obtain

$$\dot{X} + J_0(g/\Omega) \sin X = f \cos \omega t, \quad (16)$$

and the response amplitude Q is given by

$$Q = \frac{1}{\sqrt{\omega_r^2 + \omega^2}}, \quad \omega_r = |J_0|. \quad (17)$$

The stability determining quantity λ of the equilibrium points of Eq. (16) with $f=0$ are given by

$$\lambda = \begin{cases} \lambda_{\min} = -J_0, & \text{for } X_{\min}^* = 0, \pm 2\pi, \dots \\ \lambda_{\max} = J_0, & \text{for } X_{\max}^* = \pm \pi, \pm 3\pi, \dots \end{cases} \quad (18)$$

In Fig. 8, we plotted Q , ω_r , and the variation of stability determining eigenvalue λ_{\min} and λ_{\max} of the equilibrium points X_{\min}^* and X_{\max}^* , respectively, versus g . Note that Q displays a series of resonance peaks. In contrast to the underdamped system, in the overdamped system, resonances occur when $\omega_r=0$ at which the stability of the equilibrium points X_{\min}^* and X_{\max}^* are exchanged. Moreover, Q is locally minimum when ω_r becomes a maximum and λ of the stable equilibrium points is minimum (maximally stable). At all the resonance values of g , we find $Q=1/\omega$. Furthermore, for both $\omega < 1$ and $\omega > 1$, the response amplitude $Q(g) > Q(0)$ and $Q_L = 1/\omega$.

IV. VIBRATIONAL RESONANCE IN TRUNCATED PERIODIC POTENTIAL SYSTEMS

In this section, we report on the effect of the truncation of the periodicity of the periodic potential on VR. To know the role of periodicity of the potential beyond $|\theta| > 2\pi$, we consider the overdamped system with the truncated periodic potential of the form

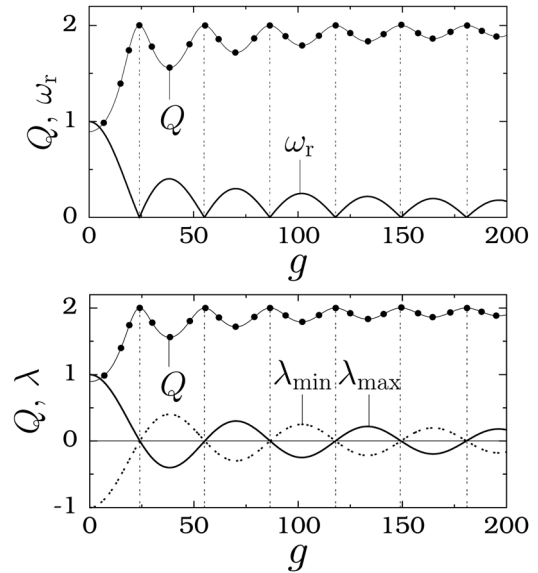


FIG. 8. Variation of theoretical Q (continuous line), numerical Q (solid circles), resonant frequency ω_r , and the eigenvalue λ of the equilibrium points X_{\min}^* and X_{\max}^* (for $f=0$) of the overdamped pendulum system as a function of the control parameter g for $\omega=0.5, \Omega=10$, and $f=0.1$.

$$V_T(\theta) = \begin{cases} -1 + \frac{1}{n}(\theta - c_1)^n, & \text{for } \theta < c_1 \\ -\cos \theta, & \text{for } c_1 \leq \theta \leq c_2, \\ -1 + \frac{1}{n}(\theta - c_2)^n, & \text{for } \theta > c_2 \end{cases} \quad (19)$$

where $c_1 = -2\pi$, $c_2 = 2\pi$, and $n=2, 4$. The choices $n=2$ and $n=4$ correspond to linear and nonlinear forces, respectively, for $|\theta| > 2\pi$. Figure 9 shows the potential $V_T(\theta)$ for $n=2$ and $n=4$. In Eq. (2), we replace $\sin \theta$ by $dV_T(\theta)/d\theta$. Now, the response amplitude Q is $1/\sqrt{\omega_r^2 + \omega^2}$, where

$$\omega_r = \begin{cases} |J_0|, & \text{for } \theta(t) \in [c_1, c_2] \\ 1 \text{ for } n=2 \text{ and } \frac{3g^2}{2\Omega^2} \text{ for } n=4, & \text{otherwise.} \end{cases} \quad (20)$$

In the pendulum system, ω_r is independent of time, while in the system with the potential V_T , it is a function of time. However, as long as $\theta(t) \in [c_1, c_2]$, the resonant frequency is $|J_0(g/\Omega)|$ and Q is identical to the system (Eq. (2)). Above a critical value of g , $\theta(t)$ visits the outside region of the interval $[c_1, c_2]$. The time spent by the system outside the above interval increases as g increases. Therefore, for very large values of g , we can approximate Q as

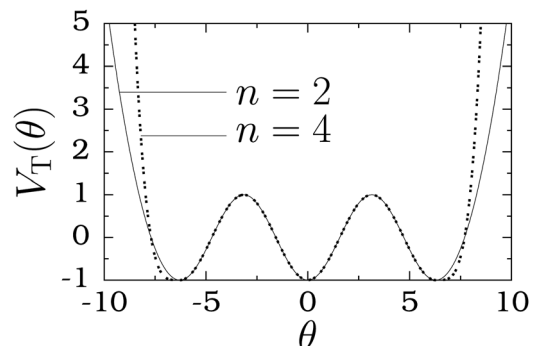


FIG. 9. Plot of $V_T(\theta)$ versus θ for $n=2$ and 4 .

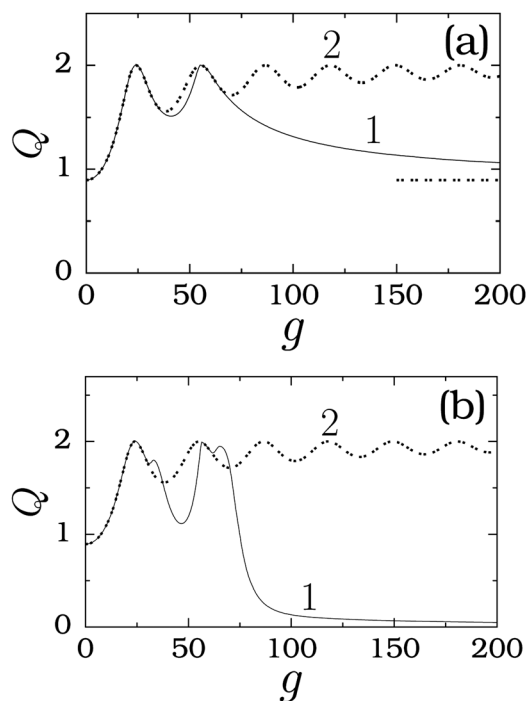


FIG. 10. Numerically computed Q versus g for the overdamped system with the truncated periodic potential (curve 1) and the overdamped pendulum system (curve 2). For the subplots (a) and (b), the values of n in the truncated periodic potential are 2 and 4, respectively. In the subplot (a), the horizontal dashed line indicates the limiting value of Q given by Eq. (21). The values of the parameters are $f=0.1$, $\omega=0.5$, and $\Omega=10$.

$$Q_L = \frac{1}{\sqrt{\omega_r^2 + \omega^2}}, \quad \omega_r = \begin{cases} 1, & \text{for } n = 2 \\ \frac{3g^2}{2\Omega^2}, & \text{for } n = 4. \end{cases} \quad (21)$$

For large values of g , the response amplitude Q becomes a nonzero constant for $n=2$ (linear force) while it decays to zero for $n=4$ (nonlinear force). The numerical Q versus g presented in Fig. 10 confirms the above results.

V. CONCLUSIONS

To conclude, we have investigated the occurrence of VR in the pendulum system for the underdamped and overdamped cases. In particular, we have analysed the impact of the presence of an infinite number of alternating stable and unstable equilibrium points. The stability of the equilibrium points around which slow oscillations occur is altered when g is varied. There are few rich features of VR in the pendulum system. In the conventional VR, $Q(g)$ decays to zero for large values of g . Different from this, in the underdamped pendulum system for $\omega < 1$, the response amplitude (Q) profile displays multiple resonance peaks, $Q(g) > Q(g=0)$ and $Q(g)$ approaches a limiting nonzero value for large values of g . Resonance occurs whenever ω_r matches with ω or it becomes locally maximum. Furthermore, at the resonance, the equilibrium points around which slow oscillations occur are maximally stable. The mechanism of VR in the overdamped system is quite different from that of the underdamped system.

In the overdamped system, the most interesting result is that $Q(g) > Q(g=0)$ for both $\omega > 1$ and $\omega < 1$ and the resonance occurs when ω_r becomes minimum ($= 0$). Another thing is that at the resonance, a transcritical bifurcation of the equilibrium points takes place. And conventional VR is found when the periodicity of the potential is truncated. Our theoretical results are clearly supported by our numerical simulations. All the features of VR in the pendulum system are explained by our theoretical approach. From the above, we believe that the study of VR in different kinds of potentials would provide further insight on VR.

ACKNOWLEDGMENTS

M.A.F.S. acknowledges financial support from the Spanish Ministry of Education and Science under Project No. FIS2006-08525 and from the Spanish Ministry of Science and Innovation under Project No. FIS2009-09898.

- ¹P. S. Landa and P. V. E. McClintock, *J. Phys. A* **33**, L433 (2000).
- ²D. Su, M. Chiu, and C. Chen, *J. Soc. Precis. Eng.* **18**, 161 (1996).
- ³V. Gherm, N. Zernov, B. Lundborg, and A. Vastberg, *J. Atmos. Sol.-Terr. Phys.* **59**, 1831 (1997).
- ⁴A. Maksimov, *Ultrasonics* **35**, 79 (1997).
- ⁵J. Victor and M. Conte, *Visual Neurosci.* **17**, 959 (2000).
- ⁶I. I. Blekhan, *Vibrational Mechanics* (World Scientific, Singapore, 2000).
- ⁷V. N. Chizhevsky and G. Giacomelli, *Phys. Rev. A* **71**, 011801(R) (2005).
- ⁸I. I. Blekhan and P. S. Landa, *Int. J. Non-Linear Mech.* **39**, 421 (2004).
- ⁹V. N. Chizhevsky, *Int. J. Bifurcation Chaos Appl. Sci. Eng.* **18**, 1767 (2008).
- ¹⁰S. Jeyakumari, V. Chinnathambi, S. Rajasekar, and M. A. F. Sanjuan, *Phys. Rev. E* **80**, 046608 (2009).
- ¹¹J. P. Baltanas, L. Lopez, I. I. Blekhan, P. S. Landa, A. Zaikin, J. Kurths, and M. A. F. Sanjuan, *Phys. Rev. E* **67**, 066119 (2003).
- ¹²S. Rajasekar, S. Jeyakumari, V. Chinnathambi, and M. A. F. Sanjuan, *J. Phys. A: Math. Theor.* **43**, 465101 (2010).
- ¹³S. Jeyakumari, V. Chinnathambi, S. Rajasekar, and M. A. F. Sanjuan, *Chaos* **19**, 043128 (2009).
- ¹⁴E. Ullner, A. Zaikin, J. Garcia-Ojalvo, R. Bascones, and J. Kurths, *Phys. Lett. A* **312**, 348 (2003).
- ¹⁵V. N. Chizhevsky, E. Smeu, and G. Giacomelli, *Phys. Rev. Lett.* **91**, 220602 (2003).
- ¹⁶V. N. Chizhevsky and G. Giacomelli, *Phys. Rev. E* **77**, 051126 (2008).
- ¹⁷C. Yao and M. Zhan, *Phys. Rev. E* **81**, 061129 (2010).
- ¹⁸B. Deng, J. Wang, and X. Wei, *Chaos* **19**, 013117 (2009).
- ¹⁹J. H. Yang and X. B. Liu, *J. Phys. A: Math. Theor.* **43**, 122001 (2010).
- ²⁰C. Jeevarathinam, S. Rajasekar, and M. A. F. Sanjuan, *Phys. Rev. E* **83**, 066205 (2011).
- ²¹J. H. Yang and X. B. Liu, *Chaos* **20**, 033124 (2010).
- ²²J. H. Yang and X. B. Liu, *Phys. Scr.* **82**, 025006 (2010).
- ²³J. H. Yang and X. B. Liu, *Phys. Scr.* **83**, 065008 (2011).
- ²⁴M. Borromeo and F. Marchesoni, *Phys. Rev. E* **73**, 016142 (2006).
- ²⁵M. Borromeo and F. Marchesoni, *Phys. Rev. Lett.* **99**, 150605 (2007).
- ²⁶L. Gammaitoni, P. Hanggi, P. Jung, and F. Marchesoni, *Rev. Mod. Phys.* **70**, 223 (1998).
- ²⁷Y. W. Kim and W. Sung, *Phys. Rev. E* **57**, R6237 (1998).
- ²⁸C. Nicolis, *Phys. Rev. E* **82**, 011139 (2010).
- ²⁹S. Saikia, A. M. Jayannavar, and M. C. Mahato e-print arXiv:1011.4198v2 [cond-mat.stat-mech] (2011).
- ³⁰P. M. Shankar, J. Y. Chapelon, and V. L. Newhouse, *Ultrasonics* **24**, 333 (1986).
- ³¹R. M. Quain, R. C. Waag, and M. W. Miller, *Ultrasound Med. Biol.* **17**, 71 (1991).
- ³²V. Mironov and V. Sokolov, *Radiotekh. Electron.* **41**, 1501 (1996).
- ³³R. Feng, Y. Zhao, C. Zhu, and T. J. Mason, *Ultrason. Sonochem.* **9**, 231 (2002).